Naval Research Laboratory

Washington, DC 20375-5320

NRL/MR/6300--13-9463

Extraction of Carbon Dioxide and Hydrogen from Seawater by an Electrochemical Acidification Cell Part IV: Electrode Compartments of Cell Modified and Tested in Scaled-Up Mobile Unit

HEATHER D. WILLAUER

Special Projects Group
Materials Science and Technology Division

DENNIS R. HARDY

Nova Research Inc.
Alexandria, Virginia

FREDERICK W. WILLIAMS

Navy Technology Center for Safety and Survivability
Chemistry Division

FELICE DIMASCIO

Office of Naval Research
Arlington, Virginia

September 3, 2013

REPORT DOCUMENTATION PAGE

Form Approved
OMB No. 0704-0188

1. REPORT DATE *(DD-MM-YYYY)*	**2. REPORT TYPE**	**3. DATES COVERED** *(From - To)*
03-09-2013	Memorandum Report	

4. TITLE AND SUBTITLE

Extraction of Carbon Dioxide and Hydrogen from Seawater by an Electrochemical Acidification Cell Part IV: Electrode Compartments of Cell Modified and Tested in Scaled-Up Mobile Unit

5a. CONTRACT NUMBER

5b. GRANT NUMBER

5c. PROGRAM ELEMENT NUMBER

6. AUTHOR(S)

Heather D. Willauer, Dennis R. Hardy,[1] Frederick W. Williams, and Felice DiMascio[2]

5d. PROJECT NUMBER

5e. TASK NUMBER

5f. WORK UNIT NUMBER
63-9189-0-2-5

7. PERFORMING ORGANIZATION NAME(S) AND ADDRESS(ES)

Naval Research Laboratory, Code 6300
4555 Overlook Avenue, SW
Washington, DC 20375-5320

8. PERFORMING ORGANIZATION REPORT NUMBER

NRL/MR/6300--13-9463

9. SPONSORING / MONITORING AGENCY NAME(S) AND ADDRESS(ES)

Office of Naval Research
One Liberty Center
875 North Randolph Street, Suite 1425
Arlington, VA 22203

10. SPONSOR / MONITOR'S ACRONYM(S)

ONR

11. SPONSOR / MONITOR'S REPORT NUMBER(S)

12. DISTRIBUTION / AVAILABILITY STATEMENT

Approved for public release; distribution is unlimited.

13. SUPPLEMENTARY NOTES

[1]Nova Research Inc., Alexandria, VA
[2]Office of Naval Research, Arlington, VA

14. ABSTRACT

An electrochemical acidification cell was scaled-up and integrated into a mobile skid design. Based on four separate evaluations of this cell, a second cell was modified to contain less ion exchange capacity in the electrode compartments. The objective of this modification was to improve the CO_2 production rate by reducing the time it takes for the effluent seawater equilibrium pH to reach 6 after a change in polarity. This report details the performance of the modified electrochemical cell as a function of pH, current, time, polarity reversal, and CO_2 and H_2 recovery. These results are compared to those measured for the original cell.

15. SUBJECT TERMS

Electrochemical acidification cell
Carbon dioxide
Hydrogen
Polarity reversal

16. SECURITY CLASSIFICATION OF:			**17. LIMITATION OF ABSTRACT**	**18. NUMBER OF PAGES**	**19a. NAME OF RESPONSIBLE PERSON**
a. REPORT	**b. ABSTRACT**	**c. THIS PAGE**			Heather D. Willauer
Unclassified Unlimited	Unclassified Unlimited	Unclassified Unlimited	Unclassified Unlimited	32	**19b. TELEPHONE NUMBER** *(include area code)* (202) 767-2673

Standard Form 298 (Rev. 8-98)
Prescribed by ANSI Std. Z39.18

CONTENTS

EXECUTIVE SUMMARY

A sea-based synthetic fuel process that combines carbon dioxide (CO_2) and hydrogen (H_2) to make jet fuel at sea is envisioned. However before such a process can become feasible, methods must be developed to extract large quantities of CO_2 and H_2 from seawater fast and efficiently. To this end, commercially available electrodeionization cells have been modified by NRL to function as electrochemical acidification cells. After the technology was successfully demonstrated in the laboratory, it was scaled-up and integrated into a mobile skid design. The electrochemical acidification cell performance was evaluated as a function of pH, current, time, polarity reversal, and CO_2 and H_2 recovery on four separate evaluations in 2011 (January 22th – 27th, April 25th – 29th, July 11th – 15th, and August 28th – Sept 1st). The results of these evaluations led to the modification of a second electrochemical acidification cell. The objective of this modification was to improve the CO_2 production rate by reducing the time it takes for the effluent seawater equilibrium pH to reach 6 after a change in polarity.

The second cell was modified to have less ion exchange capacity in the electrode compartments. The electrical resistance profiles for both cells show that cyclically reversing the polarity of the cell's electrodes minimizes the effects of mineral deposits on the electrode surface. The pH profiles illustrate that both acidification cells reduce seawater pH below 6.0. The change and reduction in ion exchange capacity for any defined current has improved the electrochemical cell's acidification performance by reducing effluent seawater equilibrium pH to 6 at a rate that increases production time of CO_2 by 33% over the original cell.

Different quantitative gas sampling analysis methods were used to measure CO_2 degassing from acidified seawater by hollow fiber membrane technology. The results of two different gas sampling methods coincided and correlated well with the method that measured $[CO_2]_T$ in seawater. The results also confirm the relationship between seawater salinity, seawater carbonate concentration, and seawater temperature on the ease of CO_2 degassing from seawater.

In addition to CO_2 analysis, gas samples collected from the cathode measured 91% in H_2 composition by on-line thermal conductivity measurements and off-line (independent contractor) gas chromatographic analysis.

EXTRACTION OF CARBON DIOXIDE AND HYDROGEN FROM SEAWATER BY AN ELECTROCHEMICAL ACIDIFICATION CELL
PART IV: ELECTRODE COMPARTMENTS OF CELL MODIFIED AND TESTED IN SCALED-UP UNIT

1.0 BACKGROUND

The feasibility of producing jet fuel at sea from environmental CO_2 and H_2 to support carrier flight operations is of interest. In-theater, synthetic fuel production is a "game changing" proposition that could offer the Navy significant logistical and operational advantages by reducing dependence on increasingly expensive fossil fuels and by reducing fuel logistic tails and their vulnerabilities resulting from fuel delivery at sea. The Navy has proposed moving to a common fuel JP5, throughout its operations [1]. Petroleum derived fuel cost and availability issues have prevented this transition so far. If the Navy does move to a single fuel this proposed process would simplify any future shipboard production of fuel. In addition, a ship's ability to produce any significant fraction of the battle group's fuel for operations would increase the Navy's operational flexibility and time on station by reducing the mean time between refueling.

Technologies currently exist to synthesize hydrocarbon fuel on land, given sufficient primary energy resources such as coal and natural gas [2]. However, these technologies are not CO_2 neutral, and they are not practical for a sea-based operation. Extracting CO_2 from seawater is part of a larger project to create liquid hydrocarbon fuel at sea [3-19].

One part of the overall program by NRL (Naval Research Laboratory) was a series of tests in the laboratory to recover CO_2 and H_2 from seawater using an electrochemical acidification cell [13, 15, 16, 19]. The objective of those studies was to determine the effects of acidification cell configuration, seawater composition, flow rate, and current on seawater pH.

Exploiting seawater's pH is an indirect approach to recovery of CO_2 in the form of bicarbonate from the equilibrium conditions of CO_2 in seawater as shown in equations 1 and 2 [20]. The protons generated in the process acidify the seawater from pH 7.8 to pH 6.0. Johnson, et al. demonstrated that when the pH of seawater is decreased to 6 or less, carbonate and bicarbonate are re-equilibrated to CO_2 gas as shown in equation 3. This method has been the basis for standard quantitative ocean $[CO_2]_T$ measurements for over 25 years [20].

$$[CO_2(g)]_{air} \overset{H_2O}{\rightleftarrows} [CO_2(aq)] \overset{H_2O}{\rightleftarrows} [H_2CO_3(aq)] \quad (1)$$

$$CO_2(g) \overset{H_2O}{\rightleftarrows} CO_2(aq) + H_2O \rightleftarrows H_2CO_3(aq) \rightleftarrows H^+ + HCO_3^-(aq) \rightleftarrows 2H^+ + CO_3^{2-}(aq) \quad (2)$$

$$HCO_3^- + H^+ \rightleftarrows H_2CO_3 \rightleftarrows H_2O + CO_2(g)\uparrow \quad (3)$$

Manuscript approved September 17, 2012.

NRL laboratory studies have shown that the acidification cell was able to decompose freshwater in the electrode compartments into hydrogen ions (H^+), hydroxyl ions (OH^-), H_2 gas, and oxygen gas (O_2) by means of electrical energy. Simultaneous and continuous ion exchange and regeneration occurred within the cell eliminating the need for regeneration by hazardous chemicals. The degree of ion exchange and regeneration within the cell was controlled by the applied current. Lowering the pH of seawater by the acidification cell was found to be an electrically driven process, where seawater pH is proportional to applied current. In addition to CO_2, the cell produced a portion of the H_2 needed for a hydrocarbon synthesis process with no additional energy penalty. The acidification cell operated in the laboratory at a seawater flow rate of 140 mL/min and both electrode compartments at a deionized water flow rate of 10 mL/min [13, 15, 16, 19].

2.0 OBJECTIVE

The objective of this phase of the overall project has been to transition the technology from the laboratory to a marine environment for the purpose of scaling-up and integrating the processes. In this environment, CO_2 and H_2 can be produced in quantities far above those achieved at the laboratory scale. The electrochemical acidification cell for this test series has been modified from the previous test series to increase CO_2 production efficiencies [18]. This cell has similar operating parameters as the original cell (minimum seawater flow rate of 0.5 gal/min (1,900 mL/min) and a minimum electrode compartment flow rate of 0.06 gal/min (230 mL/min), and the cell has been designed as an integral part of a mobile platform unit). The following key technological challenges associated with improving process efficiencies were addressed in this test series:

- Ion exchange and system regeneration upon polarity reversal
- Membrane fouling
- Mineral deposition on the electrodes (polarity reversal)
- Power requirements
- Hydrogen production
- CO_2 recovery

3.0 APPROACH

In these test series an electrochemical acidification carbon capture skid was operated at NRL's Marine Corrosion Facility in Key West, Florida to evaluate the performance of a new cell configuration. The cell was modified to have less ion exchange capacity in the electrode compartments in efforts to improve the recovery rates of CO_2 from seawater

4.0 TEST DESCRIPTION

4.1 Electrochemical Acidification Cell

A standard commercially available electrodeionization cell (Ionpure LX-X Module) was modified to function as an electrochemical acidification cell for this evaluation. Although its design is not optimized for use as an acidification cell, it has more than served the purpose in this study. A custom design will be required to optimize the existing cell's performance. In addition

a custom design will be needed for any future larger scale-up studies that will involve seawater flow rates greater than 5,700 mL/min.

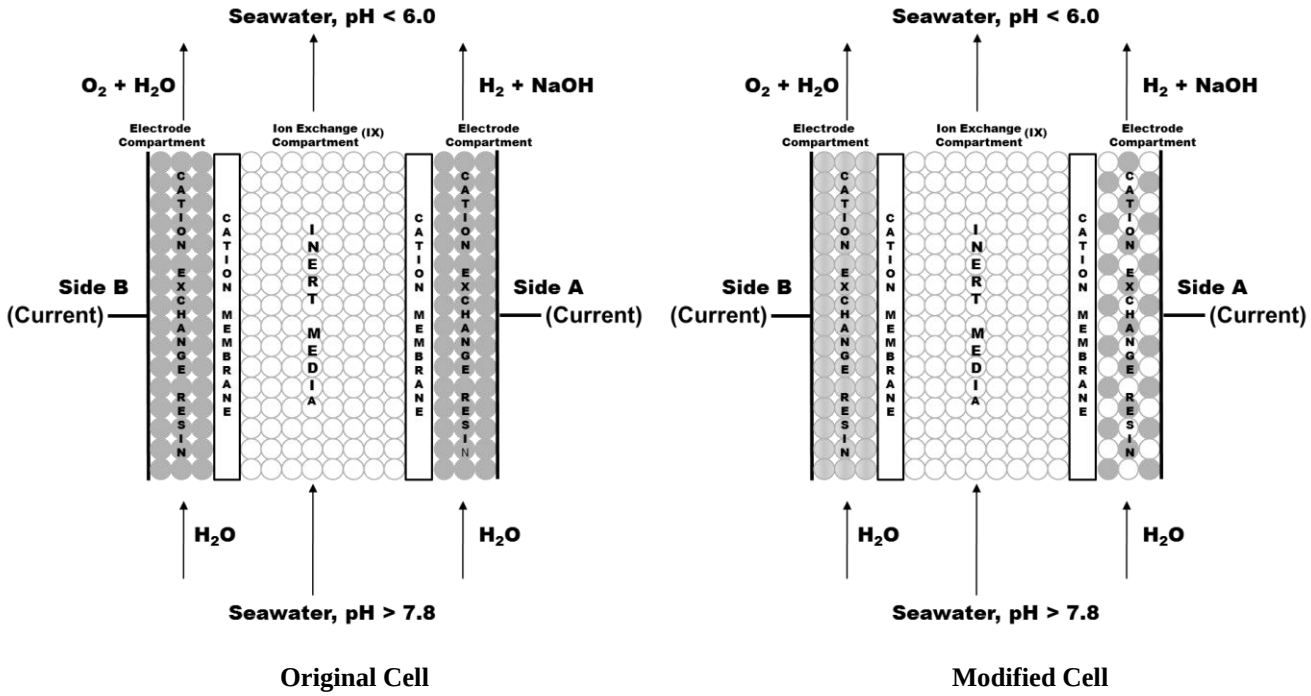

Figure 1a. Schematic of Original Electrochemical Acidification Cell and 1b. Schematic of Electrochemical of Modified Acidification Cell

The major components of each acidification cell include a central ion exchange (IX) compartment, electrode compartments (cathode and anode) and cation-permeable membranes which separate the three compartments. A cation-permeable membrane is a cross-linked polymer backbone with sulfonic acid groups attached. The acid functionality provided discrete channels for cations to migrate through the polymer matrix while blocking the passage of anions. Figure 1a and 1b compares the original acidification cell to the modified cell [18]. In the Figure both cells are composed of three compartments. Inert ceramic particles are used in the IX compartment to serve as a support structure for the membranes in both cells. In this compartment, the ions exchange in the liquid phase. In addition, Figure 1 shows that the electrode compartments contain cation exchange resin. The cation exchange resin, its amount, and capacity differ between the cells. The original cell contained 100% strong cation exchange resin from Rohm & Haas (IR-120) in both electrode compartments. Its capacity is 2.1 eq/L. In the modified cell each electrode compartment is configured to contain 50% less ion exchange capacity. However, each electrode compartment is configured differently to achieve this objective. In Figure 1, the electrode compartments of the cell are defined as side B and side A for each cell. In the second cell Figure 1b shows that side B contains 100% strong acid ion exchange resin with a capacity of 1 eq/L. Side A contains 50% less of the same strong acid cation exchange resin that was used in the original cell (2.1 eq/L). This resin is mixed with 50% inert material to fill the compartment.

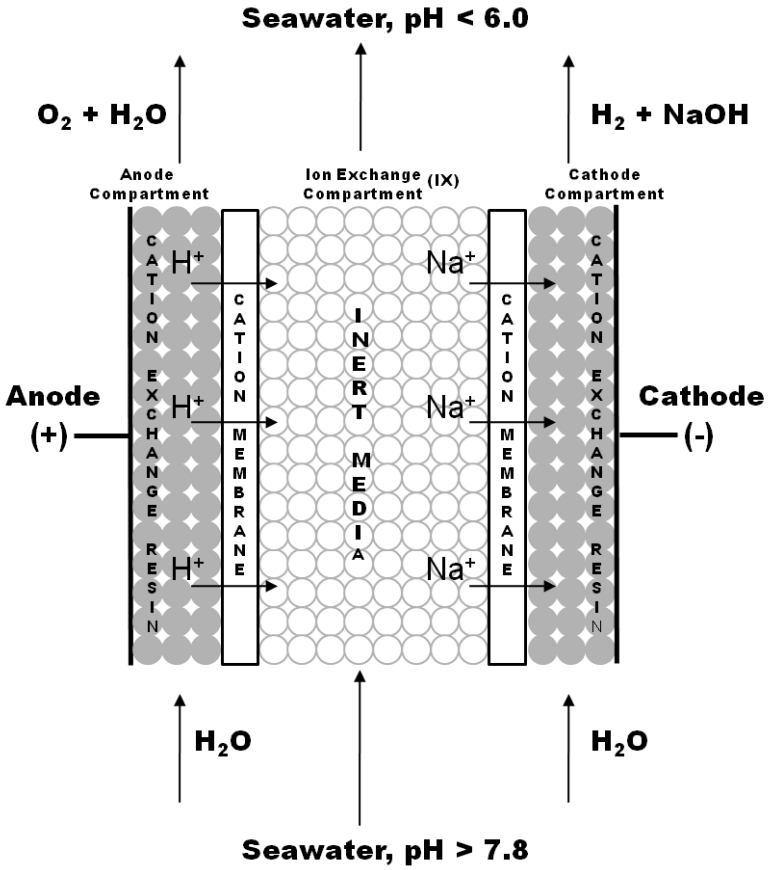

Positive ions travel through solution from anode to cathode→

Figure 2. Schematic of the Original Electrochemical Acidification Cell

Both cells in Figure 1 use direct current (DC) to exchange sodium ions (Na^+) for H^+ ions in a central stream that is flowing adjacent to two cation exchange membranes (Figure 2). For a given polarity configuration seawater is passed through the center compartment of the three compartment cell (Figures 1 and 2). Na^+ ions are transferred through the membrane closest to the cathode and removed from the seawater by means of direct current (DC) voltage (Figures 1 and 2). These Na^+ ions are replaced by H^+ ions as the current drives the ions through the membrane closest to the anode to acidify the seawater (Figures 1 and 2).

The anolyte is the water fed to the anode compartment. At the anode H^+ is generated and it must migrate from the surface of the anode, through the cation-permeable membrane, and into the IX compartment where it replaces Na^+. Therefore the anolyte was potable water so that H^+ ions are in excess and do not compete with any other cations. Water with a conductivity of less than 200 µS/cm, such as reverse osmosis (RO) permeate, is required.
The catholyte is the water fed to the cathode compartment and it must be free from hardness ions such as calcium (Ca^{+2}) and magnesium (Mg^{+2}). The pH in the cathode compartment is high

enough to precipitate these hardness ions. Therefore, a total hardness concentration of less than 50 ppm, such as RO permeate, is required. As a part of these tests, the effects of RO permeate as the anolyte and catholyte were evaluated.

Table 1 provides a detailed description of both acidification cell's electrical and flow rate specifications along with the materials used in the cell configuration. The anode and cathode are platinum-plated titanium electrodes. These tests determined the flow rate to current ratio required to lower seawater pH to the target level. This information determines electrode performance and operating life. The cell contained a polyethylene extruded cation permeable membrane. Membrane performance was evaluated during these tests, since its performance and operating life is based on current density and level of organic compounds contained in the seawater.

Table 1. Cell Configured as an Electrochemical Acidification Cell

Dimensions	
Approximate Overall Cell Dimension	33 cm x 61 cm x 16 cm
IX Compartment Width	14 cm
IX Compartment Height	35.5 cm
IX Compartment Thickness	1.8 cm
IX Compartment Volume	895 cm^3
Membranes Active Area	497 cm^2 (each)
Each Electrode Compartment Volume	214 cm^3
Electrical Specification	
Effective Electrode Active Area	497 cm^2 (each)
Max. Current Density	1,500 A m^{-2}
Flow Specification	
Max. Seawater Flow Rate	3900 mL/min
Operating Seawater Flow Rate	1900 mL/min
Max. RO Electrolyte Flow Rate	2100 mL/min
Operating RO Flow Rate	230 mL/min
Max. Operating Temperature	60 ^oC
Max. Operating Pressure	350 kPa
Materials	
Anode	Platinized Titanium
Cathode	Platinized Titanium
Membrane	Ionpure Cation-Permeable Membrane
Molded Frame and End Block	Polyethylene (PE)

4.2 Electrochemical Acidification Cell Reactions

Figure 2 shows an acidification cell exchanging Na^+ for H^+ in a stream that is flowing adjacent to two cation-permeable membranes. Direct current (DC) facilitates this exchange. Depicting seawater by sodium chloride (NaCl) and acidified seawater by HCl, the reactions within the electrochemical acidification cell are as follows:

Anode: $2H_2O \rightarrow 4H^+ + O_2 + 4e^-$ (4)

IX: $4|NaCl|_{Seawater} + 4H^+ \rightarrow 4\,Na^+ + 4|HCl|_{Acidic\ Seawater}$ (5)

Cathode: $4H_2O + 4Na^+ + 4e^- \rightarrow 4NaOH + 2H_2$ (6)

Overall: $6H_2O + 4NaCl \rightarrow 4|HCl|_{IX} + 4|NaOH| + 2|H_2|_{Cathode} + |O_2|_{Anode}$ (7)

The amount of H^+ generated by the cathode is proportional to the applied electrical current, which follows Faraday's constant. Faraday's constant is defined as the amount of electricity associated with one mole of unit charge or electron, having the value 96,487 ampere-second/equivalent.

For the anode reaction, 96,487 A-sec will produce ¼ mole O_2 gas and 1 mole H^+ and for the cathode reaction, 96,487 A-sec will produce ½ mole H_2 gas and 1 mole OH^-. This allows the amount of H^+, OH^-, H_2, and O_2 produced per amp/second of current passed through the electrodes to be derived:

Anode Reaction

$$\left(\frac{1/4\ \text{mole}\ O_2}{96{,}487\ \text{A-sec}}\right)\left(\frac{60\ \text{sec}}{\text{min}}\right) = 0.000155\,\frac{\text{mole}\ O_2}{\text{A-min}} \quad (8)$$

$$\left(\frac{1\ \text{mole}\ H^+}{96{,}487\ \text{A-sec}}\right)\left(\frac{60\ \text{sec}}{\text{min}}\right) = 0.000622\,\frac{\text{mole}\ H^+}{\text{A-min}} \quad (9)$$

Cathode Reaction

$$\left(\frac{1/2\ \text{mole}\ H_2}{96{,}487\ \text{A-sec}}\right)\left(\frac{60\ \text{sec}}{\text{min}}\right) = 0.000311\,\frac{\text{mole}\ H_2}{\text{A-min}} \quad (10)$$

$$\left(\frac{1\ \text{mole}\ OH^-}{96{,}487\ \text{A-sec}}\right)\left(\frac{60\ \text{sec}}{\text{min}}\right) = 0.000622\,\frac{\text{mole}\ OH^-}{\text{A-min}} \quad (11)$$

Therefore, for seawater with a bicarbonate (HCO_3^-) ion concentration of 142 ppm (0.0023 M) at a planned operating flow rate of 0.5 gal/min (1900 mL/min), a theoretical applied current of 7.0

amps will be required to lower the pH to less than 6.0 and convert HCO_3^- to carbonic acid (H_2CO_3) (equation 12).

$$\frac{\left(\frac{0.0023\ \text{mole}\ HCO_3^-}{\text{Liter}}\right)\left(\frac{1.89\ \text{Liter}}{\text{min}}\right)}{\left(\frac{0.000622\ \text{mole}\ H^+}{\text{A - min}}\right)} = 7.0\ \text{A} \qquad (12)$$

Removal efficiency can be defined as the ratio of the theoretical amount of CO_2 removed to the actual amount of CO_2 removed in the acidified seawater. The theoretical amount of CO_2 that can be removed from the acidified seawater is 0.0023 moles per liter. Removal efficiencies are never 100 % and can range from 50 to 95 % based on various unit operating requirements. The overall removal of CO_2 in these tests was measured to be approximately 92%.

The amount of H_2 gas generated at 7.0 A is

$$\left(\frac{1/2\ \text{mole}\ H_2}{96{,}487\ \text{A - sec}}\right)\left(\frac{60\ \text{sec}}{\text{min}}\right)(7.0\ \text{A}) = 0.0022\ \frac{\text{mole}\ H_2}{\text{min}} \qquad (13)$$

Under these conditions, the molar ratio of H_2 to CO_2 is 0.73. Increasing the current increases the molar ratio of hydrogen to carbon dioxide with no effect on the operation of the acidification cell. H^+ generated will either exchange with Na^+ in the seawater to further lower its pH or migrate through the IX compartment and into the cathode compartment where it will combine with OH^- to form water.

4.3 Carbon Capture Skid

The original acidification cell was removed from the skid and replaced by the modified cell. This cell was mounted onto a portable skid along with an RO unit, power supply, pump, carbon dioxide recovery system, and hydrogen vacuum stripper to form a carbon capture system. Figures 3 and 4 are a composite schematic and picture of the system with dimensions of 63" x 36" x 60". Figure 5 provides a block diagram that describes how the system in Figure 3 operates. The system has evolved since its initial conception and installation at NRL Key West in January of 2011, to include different carbon recovery technology and more filtration media. In addition the NRL-Key West facility has made modifications to its internal infrastructure that reduced the in-house seawater supply line pressure from 40-60 psi to 20 psi. At these pressures it was necessary to use a 70 psi 15 gallon/minute well pump to pressurize the seawater from the in house supply to pressures greater than the 20 psi needed to run the RO system. The seawater is filtered by two spin down filters in series (100 μm and 30 μm). After filtration a portion of the seawater is sent to an 11 gallon high density polyethylene container that functions as the seawater feed container. Before the seawater in the seawater feed tank is fed to the center

compartment of the acidification cell at 0.5 gallon/minute, it is pumped through a 5 μm filter cartridge. The other portion of the seawater supply is fed to the RO system for processing. The RO system is an EPRO-1000SW from Crane Environmental, Inc. (Venice, FL) that is capable of producing 0.7 gallons per minute (1000 gallons per day) of permeate (potable water quality from seawater at a conductivity of approximately 200 μS/cm). This water is stored in an 11 gallon polyethylene container that is specified as the RO feed container (Figure 3). This water is the feed water to the electrode compartments of the acidification cell at a flow rate of 0.12 gallon/minute (460 ml/min). The flow is split as it enters the acidification cell resulting in electrode compartment flow rates of 0.06 gallon/minute (230 mL/min).

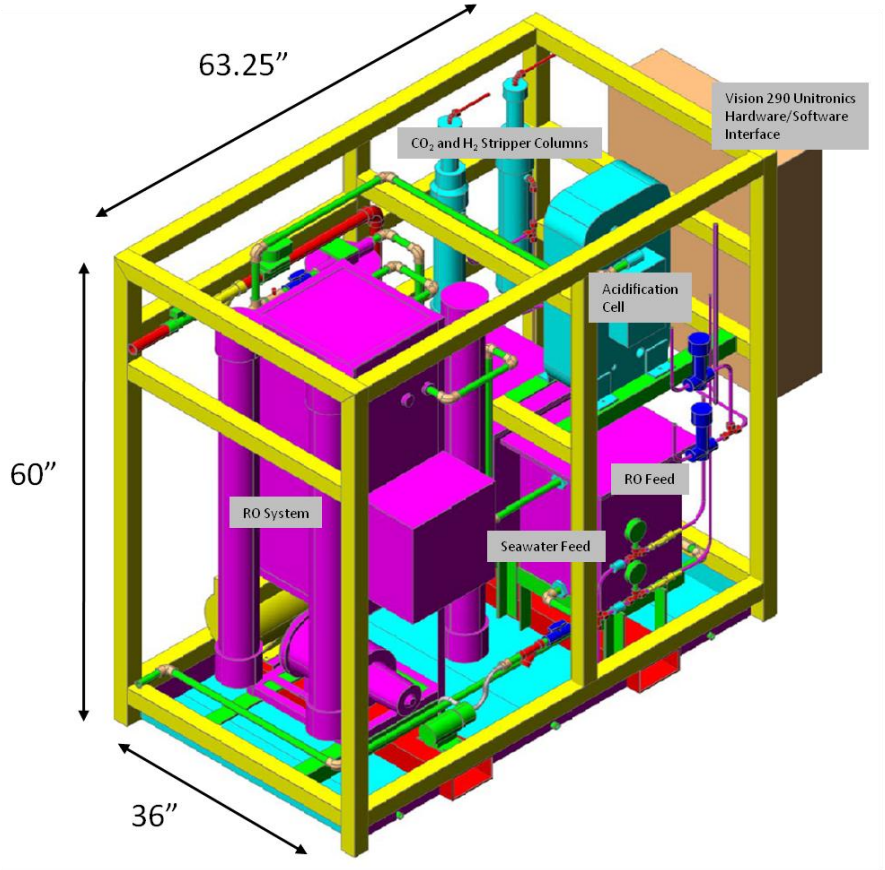

Figure 3. Composite Schematic of Carbon Capture Skid

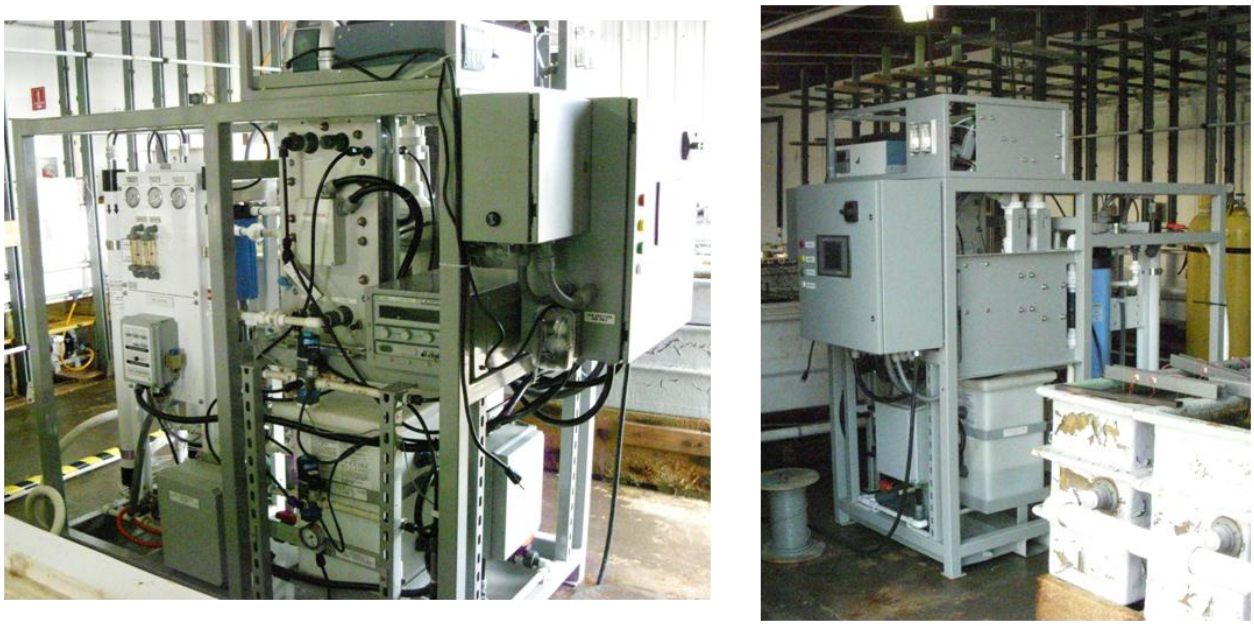

Figure 4a. Front and 4b. Back Pictures of Carbon Capture Skid at NRL Key West Facility

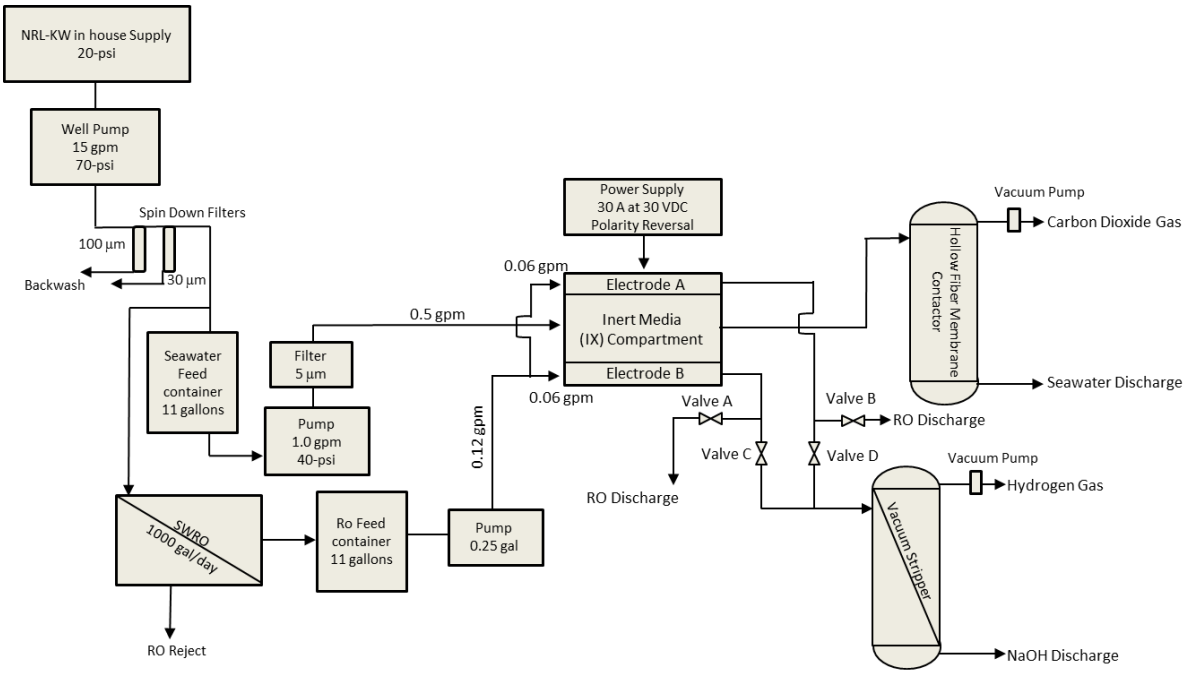

Figure 5. Block Diagram Carbon Capture Skid

Figure 5 shows that the acidification cell has been designed so that the polarity of the cell can be reversed. This reversal is essential to aid in reducing mineral deposits on the electrode that is operating as the cathode. Ions that impart hardness to seawater include calcium (Ca^{+2}) and magnesium (Mg^{+2}) ions, and their total concentration is typically less than 2,000 mg/L. Hardness ions can migrate from the seawater in the IX compartment (Figures 1, 2 and 5) or could be introduced into the cathode compartment by the water feeding the cathode compartment. In previous laboratory studies deionized water was used as the feed water to the cathode compartment, so the only hardness ions entering the cathode compartment were from the IX compartment [16, 19]. However, during these tests it was found that the electrical resistance (voltage divided by amperage) increased from 4.07 Ohms to 6.45 Ohms over 150 minutes of operation. This 58% increase in resistance was an indication that minerals (Ca^{+2} and Mg^{+2}) were depositing on the electrode surface of the cathode. These effects can be reduced by reversing the polarity of the electrodes. The change in polarity causes the minerals (scaling) to disassociate from the electrode surface. This is a common practice in Electrodialysis Reversal (EDR) processes. These processes are used to desalinate brackish ground and surface waters. Figure 5 shows that the flow from the individual electrode compartments to the hydrogen vacuum stripper are controlled by solenoid valves (valves C and D) to accommodate the necessary changes in polarity to the cell. The frequency of polarity reversal was a part of the four previous evaluations of the original cell. These parameters are specific to the IONPURE cell and therefore operating guidelines have been well established and used initially for operation of the modified cell. In this study the effects of polarity reversal on cell re-equilibration and cell performance are the primary focus.

During these tests CO_2 extraction technology was tested to verify efficient methods of liberating the CO_2 gas from the acidified effluent seawater. Specifically a 2.5 inch x 8inch Liqui-Cel polyethylene hollow fiber membrane contactor was evaluated. The $[CO_2]_T$ content of the acidified effluent seawater was measured by coulometry after contact with the different CO_2 extraction technologies to determine the efficiency of the extraction method.

In addition, the CO_2 gas liberated from the acidified seawater was measured by a standard Honeywell gas analyzer with a thermal conductivity detector. Additional CO_2 gas samples were also collected and analyzed by TRI Air Testing Inc.

During this test series a 2.5 inch x 8 inch Liqui-Cel polyethylene hollow fiber membrane contactor was evaluated for recovery of H_2 from the effluent of the cathode compartment. The H_2 gas was measured qualitatively throughout the test series by a standard Honeywell gas analyzer. In addition, H_2 gas samples were collected during testing and sent out to TRI Air Testing Inc. for independent gas analysis.

A Mastech HY3030EX 0-30 amp, 0-30 volt high-current, high-voltage regulated DC power supply controls the pH of the seawater. NRL's Marine Corrosion Facility supplied two (220 Vac, 40 A) and four (110 Vac, 20 A) electrical power feeds to power the skid.

5.0 EXPERIMENTAL

5.1 Carbon Capture Skid Operating Conditions

Table 2 provides the operating flow rate conditions for the acidification cell in these test series. Seawater flows through the IX compartment of the cell at 0.5 gal/min (1900 mL/min) (Figures 1, 2 and 5). The Table shows that at this flow rate the maximum calculated CO_2 available for extraction is 0.004 moles/min (0.0023 moles/L CO_2 (100 mg/L) x 1.89 L/min). The RO flow rate to the electrode compartments is 0.06 gal/min (230 mL/min).

Table 2. Electrochemical Acidification Cell Operating Configuration

Applied Current to Electrochemical Cell	**7 amps**	**30 amps**
Operating Seawater Flow Rate IX Compartment	**0.5 gal/min**	**0.5 gal/min**
CO_2 Concentration Extracted at 100% efficiency (eq 12)	0.0040 moles/min	0.0040 moles/min
CO_2 Concentration Extracted at 92% efficiency (eq 12)	0.0037 moles/min	0.0037 moles/min
Operating RO Flow rate to Electrode Compartments	**0.06 gal/min**	**0.06 gal/min**
H_2 Concentration Extracted at 100% (eq 13)	0.002 moles/min	0.010 moles/min
Calculated Synthetic Fuel for 100% CO_2 and H_2		0.027 gal/day

In these test series a 30 volt, 30 amp DC power supply is used to provide current to the acidification cell. Table 2 provides the operating flow rates and currents that were evaluated in the different test series and the calculated minimum amounts of CO_2 and H_2 extractable at those currents and process efficiencies of 92% and 100%. The Table shows that the maximum calculated extractable CO_2 when the cell is operating at 92% efficiency and 7 amps is 0.0037 moles/min. Thus the theoretical flow rate in mL/min to current ratio is estimated to be 270 mL/amp (equation 12). The available hydrogen at 7 amps is 0.002 moles/min. At these hydrogen concentrations, a mole ratio of 0.5:1 H_2 to CO_2 is inefficient for hydrocarbon production. During this test series the modified acidification cell was operated at 20 amps to compare and quantify the relationship between the modified cell and the original cell at a defined cell current.

There are two principle reactions that take place in the synthesis of a jet fuel fraction ($C_{11}H_{24}$) from CO_2 and H_2. In equation 14, CO_2 is reduced to CO by the reverse water gas shift reaction. Then CO is converted to a theoretical minimum hydrocarbon chain length of eleven by the Fischer-Tropsch reaction shown in equation 15 [9, 21, 22]. The sum of equations 14 and 15 result in equation 16. Equation 16 shows the mole ratio of H_2 to CO_2 is 3.1 to 1, and laboratory results indicate that this ratio is necessary for efficient hydrocarbon production.

$$11CO_2 + 11H_2 \rightarrow 11CO + 11H_2O \qquad (14)\text{ Reverse water gas shift}$$

$$11CO + 23H_2 \rightarrow C_{11}H_{24} + 11H_2O \qquad (15)\text{ Fischer Tropsch}$$

$$11CO_2 + 34H_2 \rightarrow C_{11}H_{24} + 22H_2O \qquad (16)\text{ Sum of equations 14 and 15}$$

To produce feedstock ratios of 3:1 for future hydrocarbon production the current to the cell has to be increased over 4 times to 30 amps. At this current the hydrogen concentration will increase to 0.01 moles/min (equation 13), and the current to flow rate ratio will be decreased from 270 mL/amp to 63 mL/amp. From equations 14 through 16 and the calculated moles/min of CO_2 and H_2 given in Table 2 when the cell is operating at 30 amps, the maximum amount of synthetic $C_{11}H_{24}$ that could theoretically be produced in this apparatus is 0.027 gallons/day (2×10^{-5} gallons/minute or 4.5 mls/hour).

The electrochemical cell was operated at a recovery of 81%. The term "recovery" is used to define the ratio of product quantity (influent seawater flow rate, 0.5 gal/min) over the total feed quantity to the cell (influent seawater flow rate and influent deionized flow rate, 0.62 gal/min) as a percent. A high recovery allows the size of the filtration unit along with the energy requirements for the unit to be minimized. This high recovery is possible due to the RO system and the ability to change the polarity of the electrodes in efforts to reduce scaling on the electrodes from hardness ions.

5.2 Carbon Dioxide and Hydrogen Gas Analysis

A UIC Coulometric system (UIC Inc, Joliet, IL 60436) [20] was used to measure the $[CO_2]_T$ content of the seawater throughout these tests. The $[CO_2]_T$ content of the seawater before acidification was measured to be approximately 100 mg/L.

TRI Air Testing Inc performed separate evaluations of gas samples of CO_2 and H_2 collected during the test evaluation.

A Honeywell 7866 digital gas analyzer with a thermal conductivity detector was used to measure the amount of H_2 gas from 2.5 inch x 8 inch Liqui-Cel polyethylene hollow fiber membrane contactor throughout the different tests.

5.3 Seawater pH

The seawater pH was monitored continuously using a standard combination electrode as it exits the CO_2 IX compartment of the cell. The seawater pH changes as a function of current applied to the electrochemical acidification cell.

5.4 Safety

Safety is paramount in all field operations. Since hydrogen was produced during these test series, it was constantly diluted with air below its lower flammability and explosive limit, before venting.

6.0 RESULTS AND DISCUSSION

The NRL team operated the electrochemical acidification carbon capture skid to evaluate, measure, and optimize a newly configured electrochemical acidification cell. The modified electrochemical acidification cell's performance was measured as a function of current, pH, time, polarity reversal, and CO_2 and H_2 production and recovery. These data are compared to the data

obtained for the original electrochemical cell [18]. These data provide insight into scaling and optimizing the performance of the system.

6.1 Electrochemical Acidification Cell Performance

The average performance data measured for the modified and the original electrochemical acidification cell during this evaluation at NRL Key West are summarized in Tables 3 and 4. The Tables provide the average measured values of the effluent seawater pH, current, voltage, and resistance as a function of time during each polarity cycle. Since each electrode compartment is filled with a different type and amount of ion exchange material it is critical to evaluate the performance of both electrodes as they cyclically change between functioning as the cathode and anode. The Tables indicate which compartment was functioning as the cathode during the cycle. During each polarity cycle, the cell was operated at the highest processing flow rate of 0.5 gallons/minute (1900 mL/min) of seawater. Between cycles the electrode compartments were flushed with RO water for a defined period of time. The flush cycle is needed to wash the excess H_2, NaOH, O_2 and H^+ from the electrode compartments before the polarity is reversed.

Table 3. The average measured values of effluent seawater pH, cell current, voltage, and resistance as a function of time using the modified cell during consecutive 45 minute polarity cycles at an applied cell current of 20 amps.

Time (minutes)	Amps	Volts	Resistance	pH	Conductivity	Polarity
0	18.2	30.5	1.69	6.63	0.0021	A
5	16.7	31.0	1.87	8.21	0.0019	A
10	17.4	31.0	1.80	7.58	0.0020	A
15	19.9	30.2	1.52	6.82	0.0024	A
20	20.0	27.9	1.40	6.29	0.0026	A
25	20.0	26.6	1.33	5.10	0.0027	A
30	20.0	25.8	1.30	3.90	0.0028	A
35	20.0	25.8	1.29	3.54	0.0028	A
40	20.0	25.8	1.29	3.40	0.0028	A
45	20.0	26.3	1.31	3.32	0.0028	A
0	20.0	29.5	1.48	7.47	0.0024	B
5	18.0	31.0	1.73	8.04	0.0021	B
10	18.0	31.0	1.73	7.93	0.0021	B
15	19.4	31.0	1.60	7.11	0.0023	B
20	20.0	30.2	1.51	6.15	0.0024	B
25	20.0	29.4	1.47	4.55	0.0025	B
30	20.0	29.0	1.48	3.77	0.0025	B
35	20.0	28.8	1.44	3.43	0.0025	B
40	20.0	28.7	1.43	3.32	0.0025	B
45	20.0	29.0	1.45	3.28	0.0025	B

Table 4. The average measured values of effluent seawater pH, cell current, voltage, and resistance as a function of time using the original cell during consecutive 45 minute polarity cycles at an applied cell current of 20 amps.

Time (minutes)	Amps	Volts	Resistance	pH	Conductivity	Polarity
0	20	18.9	0.92	7.57	0.0039	A
5	20	20.0	0.97	7.84	0.0037	A
10	20	21.0	1.04	7.74	0.0035	A
15	20	21.1	1.04	7.72	0.0035	A
20	20	21.1	0.99	7.13	0.0037	A
25	20	19.3	0.96	6.49	0.0038	A
30	20	18.7	0.93	5.34	0.0039	A
35	20	18.3	0.91	3.31	0.0040	A
40	20	18.2	0.90	2.91	0.0040	A
45	20	18.1	0.90	2.91	0.0040	A
0	20	1.01	1.01	6.48	0.0036	B
5	20	0.99	0.99	6.68	0.0036	B
10	20	1.04	1.04	7.76	0.0035	B
15	20	1.03	1.03	7.63	0.0035	B
20	20	0.98	0.98	7.28	0.0037	B
25	20	0.94	0.94	6.73	0.0038	B
30	20	0.90	0.90	5.95	0.0040	B
35	20	0.87	0.87	4.23	0.0041	B
40	20	0.85	0.85	2.93	0.0043	B
45	20	0.85	0.85	2.98	0.0042	B

6.1.1 Seawater pH Profiles as a Function of Applied Cell Current over Time

In these studies Polarity A and B define the electrode compartment side of the cell (side A or B) from Figures 1a and 1b that is functioning as the anode during each cycle. Figure 6 compares seven pH profiles measured as a function of time for Polarity A at an applied cell current of 20 Amps. The electrode compartment acting as the anode during these 7 cycles was filled with a mixture containing 50% cation exchange resin with a capacity of 2.1 eq/L and 50% inert material. The cathode compartment was filled with cation exchange resin with a capacity of 1.0 eq/L. The initial pH of the influent Key West seawater during this evaluation was 8.18 ± 0.02.

The Figure shows that after approximately 20 minutes have passed the pH of the effluent seawater dropped below 6. This is a function of the cation exchange resin capacity, volume (215 cm^3), and applied current. After 26 minutes the pH of the effluent seawater measured below 4. Previous results indicate that 92% of the CO_2 is recoverable at a seawater pH below 4.5 [13, 15, 16, 19].

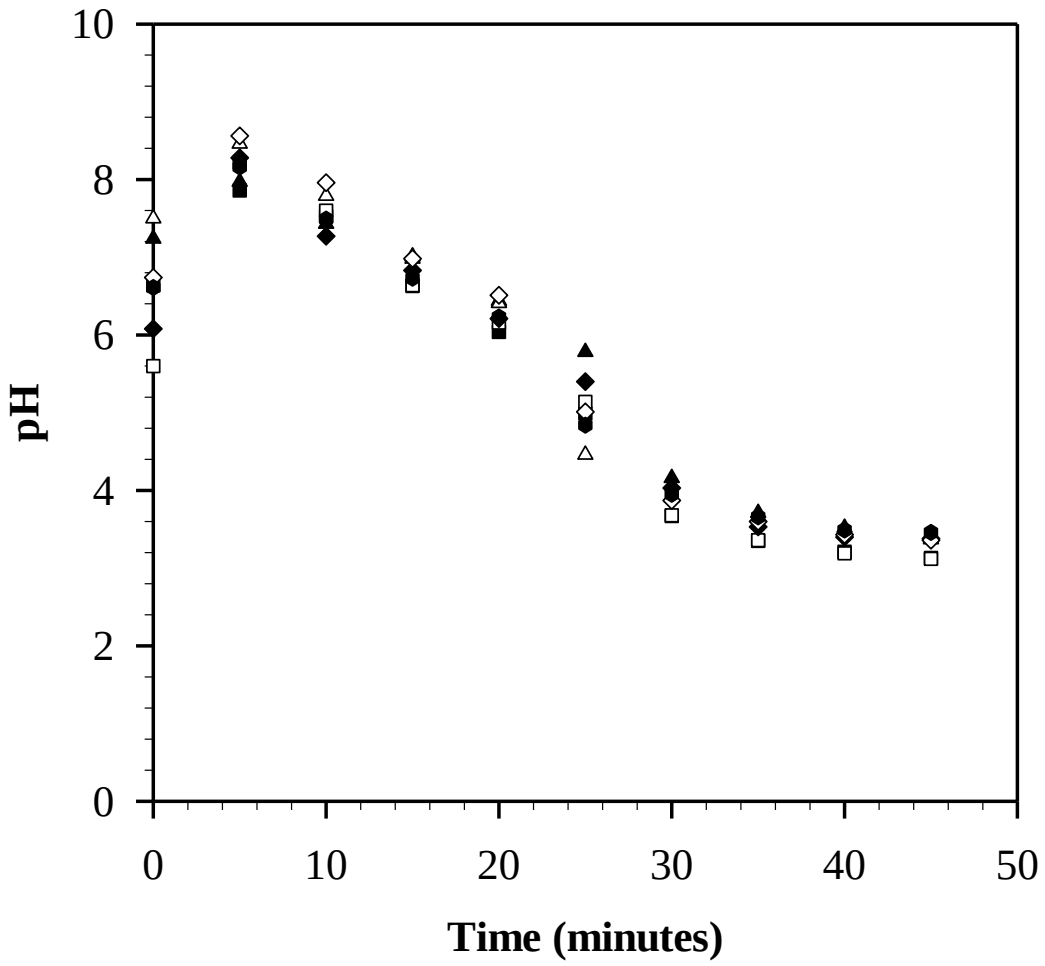

Figure 6. A pH profile comparison of seven polarity cycles at 20 amps as a function of time, 45 minute cycle, polarity A.

Figure 7 shows that similar pH profiles are measured as a function of time for Polarity B at an applied cell current of 20 Amps. During these cycles the compartment acting as the anode contained 100% cation exchange resin with the capacity of 1 eq/L. These results verify that two completely different approaches of reducing the ion exchange capacities in the electrode compartments reduced the seawater pH below 6.

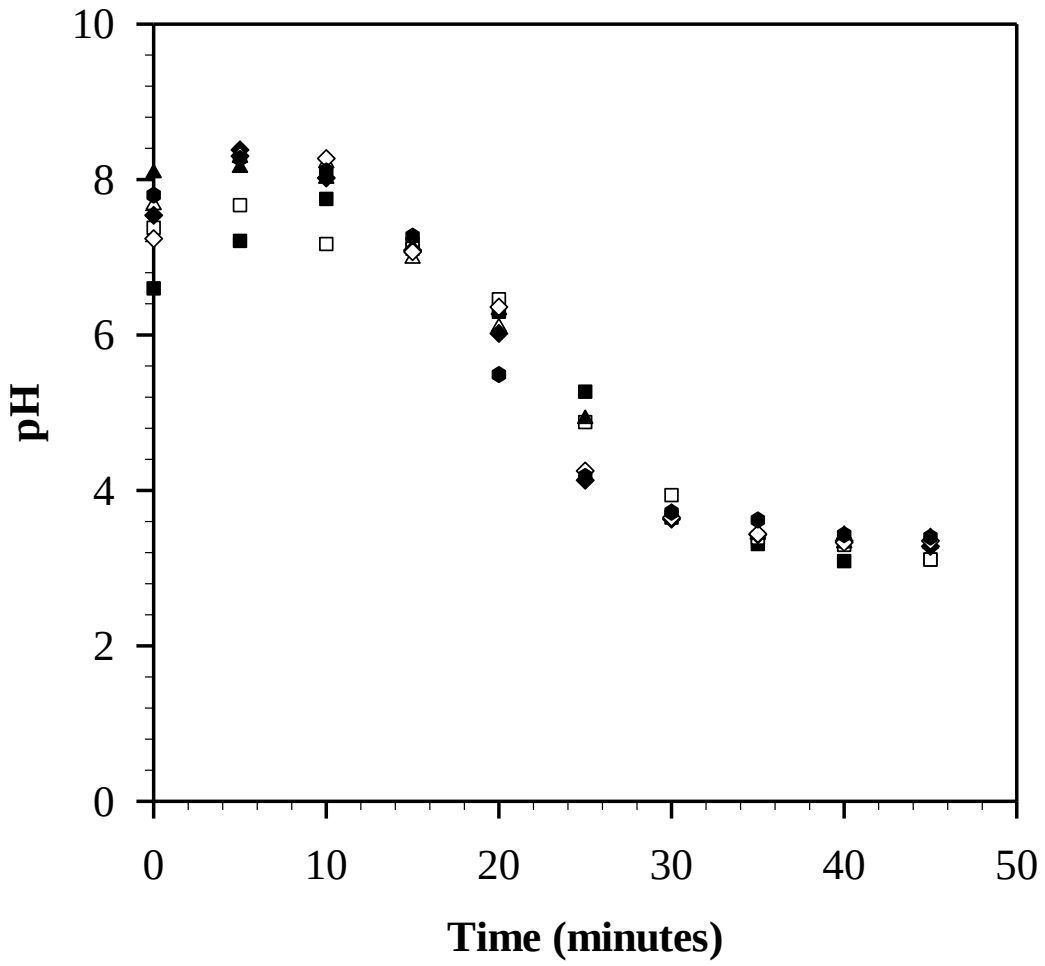

Figure 7. A pH profile comparison of seven polarity cycles at 20 amps as a function of time, 45 minute cycle, polarity B.

The objective of this test series was to increase the CO_2 production efficiency of the cell by reducing the time needed after polarity reversal for the ion exchange resin in the electrode compartments to re-establish equilibrium conditions. When the polarity is reversed, the ion exchange resin in the electrode compartment functioning as the anode is in the sodium Na^+ form, the H^+ ions generated at the anode exchange on the resin and releases the Na^+ ions. The Na^+ ions then migrate through the cation exchange membrane and into the IX compartment. The migrating Na^+ ions pass through the cation exchange membrane at the electrode now acting as the cathode and exchange on the resin to convert all the resin in that compartment to the sodium form. Equilibrium conditions are re-established during the polarity cycle when all the resin in the compartment now acting as the anode is regenerated back into the hydrogen form and all the resin in the cathode is regenerated back into the sodium form. Figures 6 and 7 show that at 5 minutes and 20 amps for all 14 cycles, the ion exchange material in the electrode compartments reach equilibrium or a level of regeneration, allowing more H^+ ions to pass through the membrane closest to the anode to acidify the seawater. This characteristic is specific to the IONPURE cell used in this evaluation. As a result the pH of the effluent seawater drops. Since the amount of H^+ ions generated from the oxidation of water on the electrode functioning as the

anode is proportional to the applied electrical current, the higher the current the faster the cell will reach a state of equilibrium. The pH profiles in Figures 6 and 7 are averaged for a given polarity and compared to the average profiles obtained for the original electrochemical acidification cell. Figure 8 shows that for a defined current the electrochemical cell's acidification reduces the effluent seawater equilibrium pH to 6 at a rate that increases production time of CO_2 by 33% over the original cell. Therefore a reduction in ion exchange capacity allows the equilibrium conditions to be re-established faster in the cell. This increase in production is crucial to the overall feasibility of scaling and utilizing the process for carbon capture from seawater.

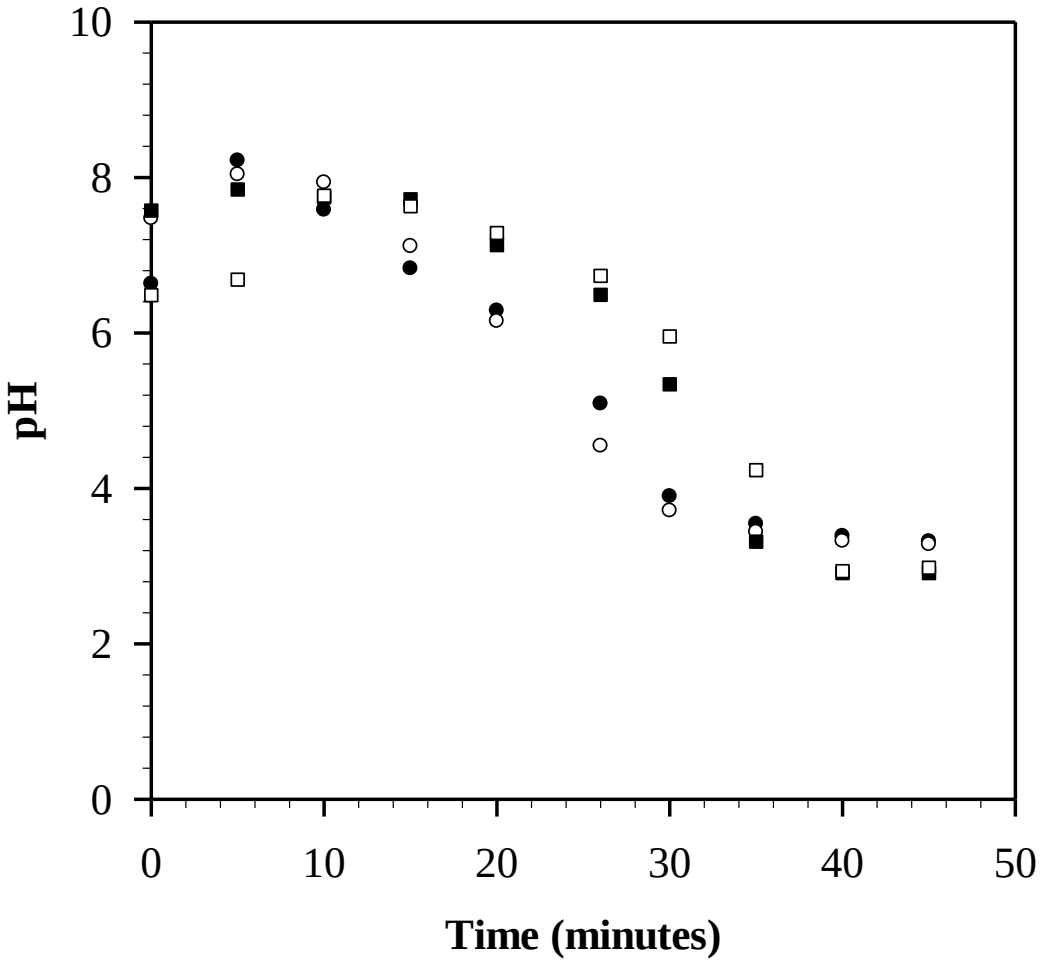

Figure 8. Average pH profiles for the original cell as a function of time, polarity A (■) and polarity B (□) compared to the modified cell, polarity A (●) and polarity B (○)

6.1.2 Electrical Resistance as a Function of Time and Applied Cell Current

An increase in electrical resistance as a function of time is a sign of hardness scaling on the cathode. Scaling (mineral deposits) takes place at the high-pH surface of the cathode. The formation of mineral deposits decreases the electrode surface area causing an increase in the electrical resistance of the entire cell. This in turn leads to a reduction in current efficiencies

and could cause a pressure drop in the electrode compartment functioning as the cathode. By cyclically reversing the polarity of the cell's electrodes, the mineral deposits will be reduced on the electrode that was operating as the cathode in the previous cycle.

Evaluation of the electrical resistance (voltage divided by amperage) of the original cell on 4 separate occasions in 2011 found that the resistance in the cell varied between test series, but the overall resistance profiles, and re-equilibration times remained consistent (Figure 9).

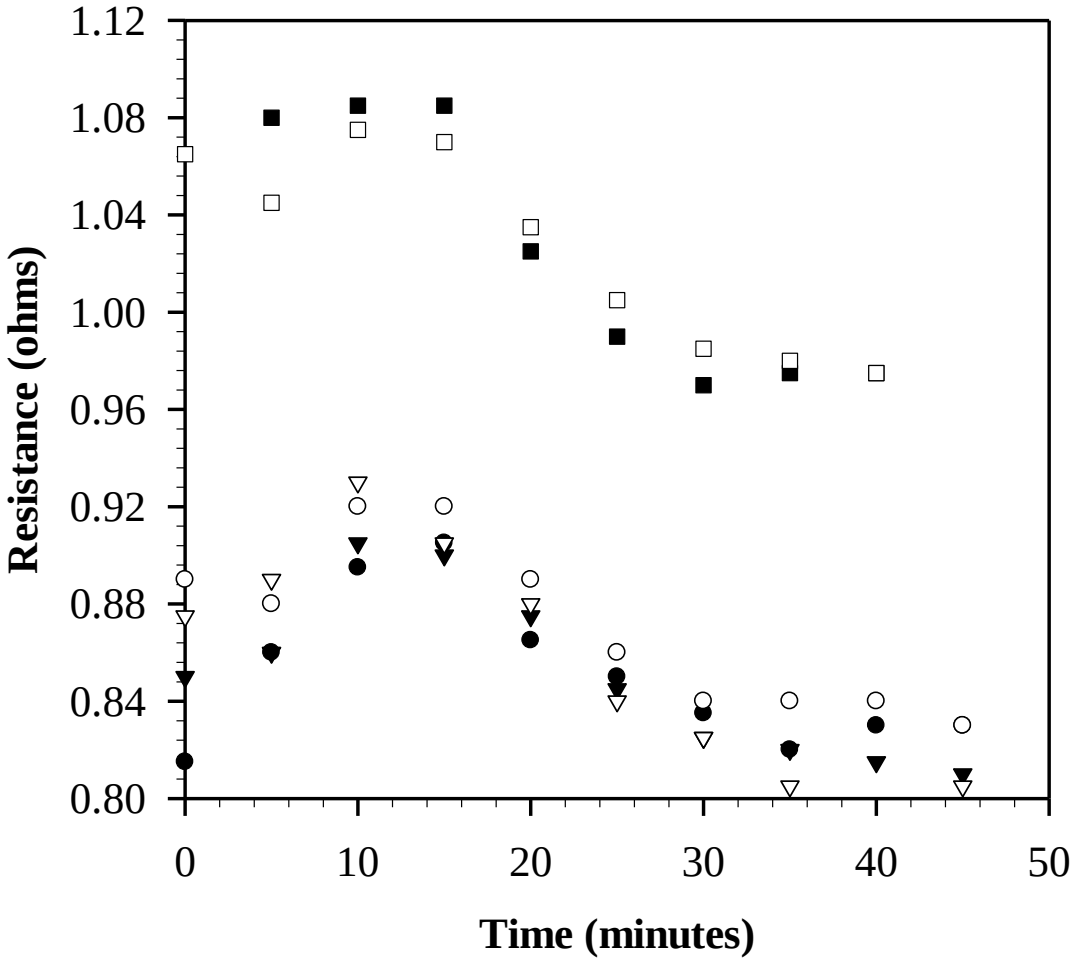

Figure 9: A electrical resistance profile comparison of six polarity cycles measured for the original cell at 20 amps as a function of time, January 2011 [40 minute cycle, polarity A (□), polarity B (■)], April 2011 [45 minute cycle, polarity A (●), polarity B (○)], August 2011 [45 minute cycle, polarity A (▼), polarity B (▽)]

The Figure indicates that the resistance of the cell does not decrease until approximately 20 minutes into the cycle. This phenomenon is also attributed to the equilibrium conditions in the cell. At lower applied cell current, fewer H^+ ions are produced at the anode, therefore it takes longer for equilibrium conditions of the cation exchange material to re-establish in both electrode compartments. The difference in the measured electrical resistance between the test series was

attributed to the bulk temperature of the influent seawater and its increase in salinity with increase in seawater temperature. A standard IONPURE module's resistance will change by approximately 2% per 1 degree Celsius change in water temperature. As water temperature increased, the electrical resistance in the cell decreased. The average seawater temperature in January, April, and August was 22 ^{o}C, 26 ^{o}C, and 31 ^{o}C. From the results, operational times were ascertained in order to provide operational parameters for IONPURE cell at any applied cell current.

Figure 10 compares the average of 7 electrical resistances profiles as a function of time for Polarity A and B of the modified cell. Comparing the averages of both cycles shows that the measured resistance decreases by approximately 31% for Polarity A and only 20% for Polarity B over the first 45 minutes of the cycle. Both cycles also indicate an increase in resistance 45 minutes into the cycle. This is consistent with results found for the original cell. The greater decrease in electrical resistance during Polarity A may be explained by the conductivity of the ion exchange resin in the electrode compartment acting as the anode.

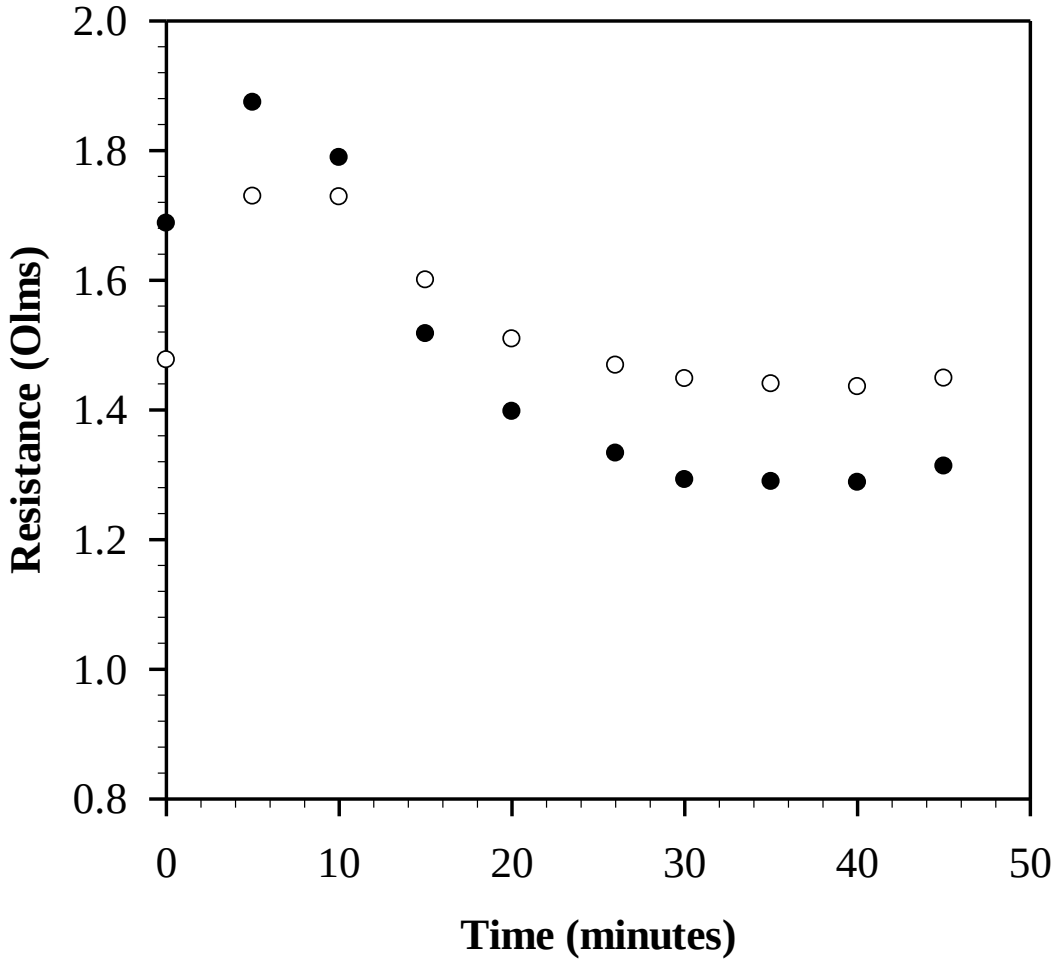

Figure 10: Average electrical resistance profile comparison of seven polarity cycles measured for the modified cell at 20 amps as a function of time, 45 minute cycle, polarity A (●), 45 minute cycle, polarity B (○).

The conductivity (κ) in the cell is the sum of all the individual components involved in ion transport. Figure 11 shows a total of 5 components responsible for the conductivity of both the original cell and the modified cell. The sum of these components is given in equation 17

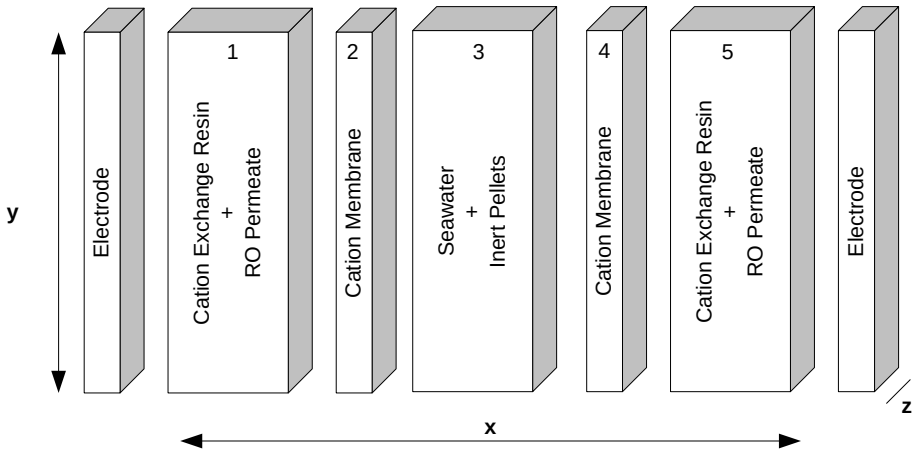

Figure 11: Electrochemical components that affect the overall conductivity of the cell

$$\kappa = \kappa_1 + \kappa_2 + \kappa_3 + \kappa_4 + \kappa_5 \qquad (17)$$

where κ_1 and κ_5 are the conductivities of the cation exchange resin and reverse osmosis permeate mixture in the electrode compartments, κ_2 and κ_4 are the conductivity of the cation exchange membranes, and κ_3 is the conductivity of the seawater and inert pellet mixture in the center compartment.

κ_1 and κ_5 are dependent on the characteristics of the cation exchange resin, particularly ion exchange capacity and DVB (divinyl-benzene) crosslinkage percentage. This will vary from one ionic form to another. κ_2 and κ_4 are fairly constant, while κ_3 is dependent on the ratio and particle size of the inert pellets. The electrical resistance 'R' (Ω) is related to the conductivity of the cell by equation 18

$$R = x/A\kappa \qquad (18)$$

where x is the distance between the electrodes in cm and A is the electrode effective area in cm^2. The area A may be expressed as a function of the electrode length (y) and width (z) as given in equation 19 and provided in Table 1 as the effective electrode active area.

$$A = (y)(z) \quad (19)$$

The electrical resistance of the cell is monitored as a function of the current and voltage supplied to the cell during a defined polarity cycle. Table 3 is the calculated average conductivity values for Polarity A and B over 7 cycles. The Table indicates that during Polarity A the ion exchange material in the anode becomes more conductive at an average of 15 minutes into the cycle. At this point the pH begins to fall below 6 and all the ion exchange material is regenerated back into the hydrogen form and all the resin in the cathode compartment is regenerated back into the sodium form. The conductivity reaches a maximum of 0.0028 at an average of 30 minutes into the cycle.

Similarly during Polarity B the ion exchange material in the anode becomes more conductive at an average of 15 minutes into the cycle. The conductivity is initially higher in this compartment upon polarity reversal, but only reaches a maximum of 0.0025 at 25 minutes. The difference in conductivity found between each polarity cycle indicates that the 50/50 mixture of cation ion exchange resin (2.1 eq) and inert material has the most conductivity and produces the least amount of resistance in the cell over an average 45 minute cycle. This decrease in resistance results in a 7% increase in power efficiency over the average 45 minute cycle. Thus the average power during Polarity A is 540 watts compared to 581 watts during Polarity B.

Figure 9 provides data that shows a change in the original cells operational performance with seawater temperature and salinity. As a result, the original cell was tested during this study to establish a set of baseline conditions for cell comparison. Table 4 provides the average amps, volts, resistance, pH, and conductivity, of two polarity cycles (Polarity A and B) measured for the original cell.

Figure 12 compares the average resistance as a function of time of the original cell and the modified cell. Figure 12 shows the average resistance for both polarity cycles of the original cell is approximately 0.96. This value is 35% less than the average resistance of the modified cell during Polarity A (50/50 ion exchange and inert material) and 37% less than the average resistance of Polarity B (50% less ion exchange capacity 1.0 eq/L). The greater resistance in the modified cell is a result of the conductivity of the ion exchange material in the electrode compartments. The average conductivity of the original cell shown in Table 4 is 0.0038 compared to 0.0024 of the modified cell. This 37% reduction in conductivity results in a 37% increase in cell resistance. This increase in cell resistance results in an increase in the average power requirements from 387 watts needed for the original cell to 540 watts (Polarity A) and 581 watts (Polarity B) needed for the modified cell.

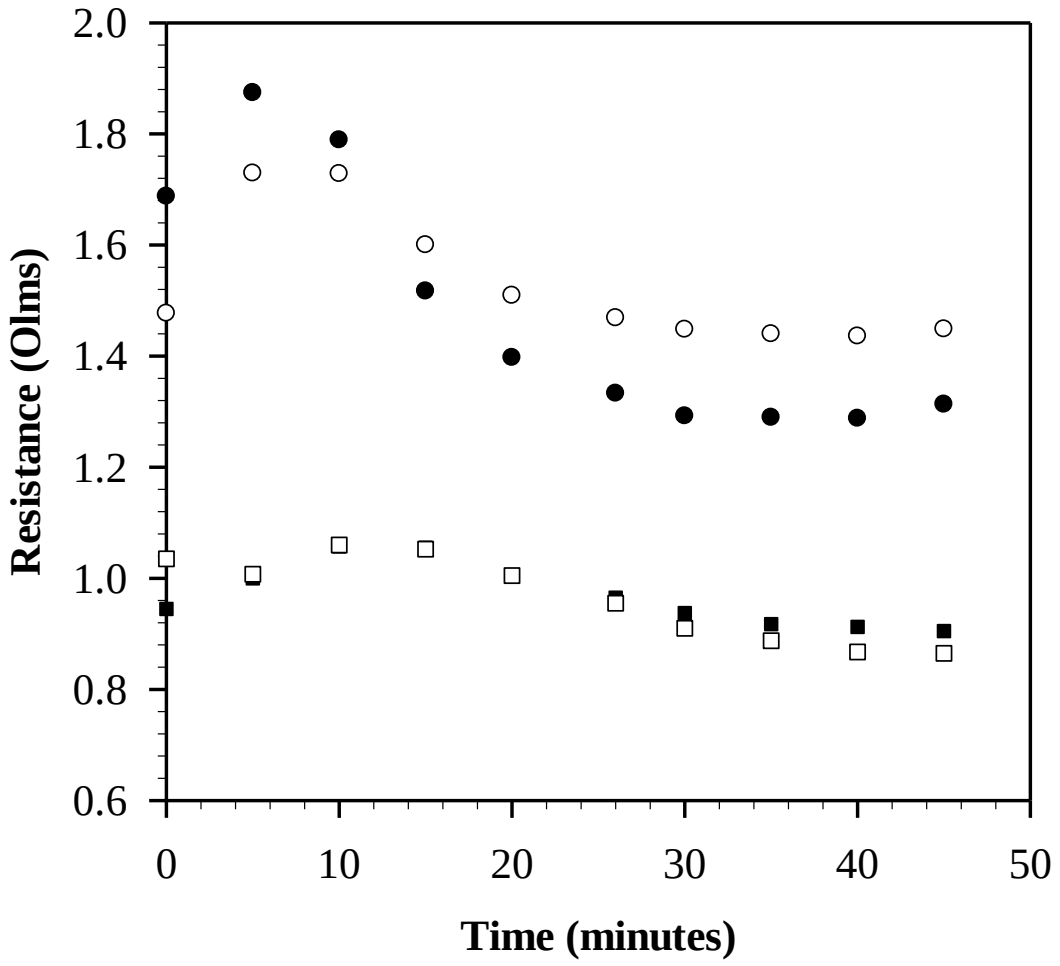

Figure 12: Average electrical resistance profiles as a function of time measured for the original cell and the modified cell at 20 amps and 45 minute cycles, modified cell polarity A (●), polarity B (○), original cell polarity A (■), polarity B (□).

6.2 Carbon Capture Analysis

NRL has recently ascertained from both the laboratory feasibility tests and scaled-up evaluations that seawater more readily degasses from seawater solutions higher in salt concentration and carbonate concentration at pH below 6. In Table 5 the results are given for three separate evaluations of the electrochemical process at NRL Key West. The first evaluation of the scaled-up carbon captures system found that approximately 48% of the $[CO_2]_T$ spontaneously degassed from the effluent seawater at pH 3.63. Further improvements in degassing the seawater were not achieved using different stripper columns to produce larger surface area for seawater degassing by a 600 mL/min vacuum pump operating at a vacuum of 12 inches of Hg.

During the April 2011 evaluation a Liqui-Cel polyethylene hollow fiber membrane contactor was tested as a method to increase seawater surface area and thus improve in CO_2 degassing

efficiency from the seawater at pH below 6. Table 5 shows $[CO_2]_T$ degassing between pH 3 and 4 increased from 48% to 92%. Since the CO_2 gas recovered is contaminated by the oil in the rotary vane pump, a diaphragm pump capable of 25 to 30 inches of Hg was purchased and used in the January 2012 evaluations of $[CO_2]_T$ recovery. During the evaluation it was found that only 63 to 66% of $[CO_2]_T$ could be recovered using a vacuum of approximately 29.1 inches of Hg. This percentage was improved to 85% when the vacuum was increased to 30.5 inches of Hg using a rotary vain pump.

Table 5. CO_2 Degassed Samples from Acidification of KW seawater

Seawater pH	**Vacuum Pump Type**	**Vacuum pressure inches Mercury**	**(%) CO_2 by Coulometery**	**(%) CO_2 in Gas Sample by TCD (onsite)**	**(%) CO_2 in Gas Sample (Independent Evaluations)**
January 2011					
8.03			100		
3.63			48		
April 2011					
8.26		Blank (no vacuum)	100		
3.82	Rotary Vain	30	92		
January 2012					
8.18		Blank (no vacuum)	100		
3.67	diaphragm	29.1	63	66	
3.46	diaphragm	29.1	66	63	
3.44	diaphragm	29.1			65
3.66	diaphragm	29.1			63
3.81	Rotary vain	30.5	85		

The difference $[CO_2]_T$ recovery between the months of January and April may be explained by the decrease in seawater salinity as a function of decrease in seawater temperature. Figures 9 and 13 illustrate the difference in resistance between the different tests series conducted in January, April, and August. The greatest difference in resistance profiles is shown for the data measured in the month of January 2011 and 2012. At lower seawater temperatures the electrical conductivity of the seawater decreases as the salinity decreases due to the lack of evaporation of the surface waters at colder temperatures. This leads to an increase in the electrical resistance within the cell. In addition, under these conditions greater seawater surface area and greater vacuum requirements are needed for better CO_2 degassing efficiencies.

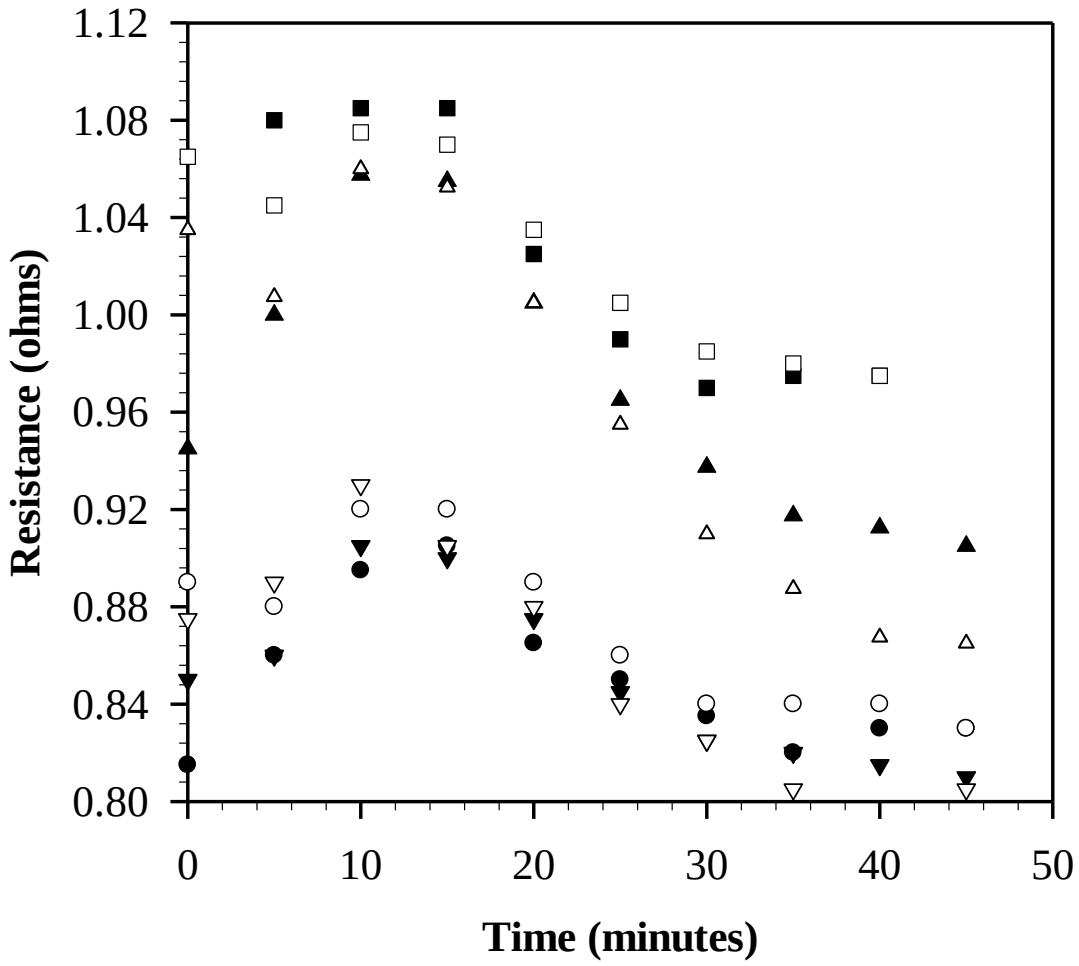

Figure 13: A electrical resistance profile comparison of five polarity cycles measured for the original cell at 20 amps as a function of time, January 2011 [40 minute cycle, polarity A (□), polarity B (■)], April 2011 [45 minute cycle, polarity A (●), polarity B (○)], August 2011 [45 minute cycle, polarity A (▼), polarity B (▽)], January 2012 [45 minute cycle, polarity A (▲), polarity B (Δ)].

In addition to measuring $[CO_2]_T$ content of seawater by coulometery during this evaluation, a Honeywell 7866 digital gas analyzer with a thermal conductivity detector was used to measure the amount of $[CO_2]_T$ gas evolved from the membrane contactor at 29.1 inches of Hg. From the table, the $[CO_2]_T$ content measured in the gas samples for a given pH of 3.67 and 3.46 was 66% and 63% respectively. Similarly the seawater samples collected at those pH measured a loss of $[CO_2]_T$ of 63% and 66% by coulometery. These results indicate an excellent correlation between two different measuring techniques of $[CO_2]_T$ content. To further substantiate these results, gas samples were collected at 3.44 and 3.66 and sent to TRI Air Testing Inc. The Table 5 shows their analysis strongly supports results found by real time gas analysis and coulometery at seawater pH less than 4.

6.3 Hydrogen Capture Analysis

During this test series a Liqui-Cel polyethylene hollow fiber membrane contactor was tested as an alternative method to the original gas stripper column for continuous removel of the hydrogen gas from the catholyte solution exiting the cathode compartment. As the catholyte flowed over the membrane contactor a 600 mL/min vacuum pump operating at a vacuum of 12 inches of Hg was used to remove the hydrogen from the catholyte stream. The gas samples collected were evaluated by TRI Air Testing Inc and found to contain 91% hydrogen by gas chromatographic analysis. Under similar conditions, hydrogen was measured to be 85% by real-time gas analysis during this evaluation.

7.0 CONCLUSIONS

Based on the evaluation of the original electrochemical acidification cell performance, a second cell was modified to contain less ion exchange capacity in the electrode compartments. The evaluation of this new design found CO_2 production increased by 33% by reducing the amount of time it takes for the effluent seawater equilibrium pH to reach 6 after a change in polarity. Evaluation of the resistance profiles and conductivity of the materials used in the electrode compartments found that the 50/50 mixture of cation ion exchange resin (2.1 eq) and inert material has the most conductivity and produces the least amount of resistance in the cell. This decrease in resistance results in a 7% increase in power efficiency over a cycle. Comparing the resistance profiles and conductivity of both the original cell and the modified cell shows that the original cells requires less average power to operate over a polarity cycle.

Quantitative measurements of $[CO_2]_T$ degassed from seawater correlated well with the quantitative difference in $[CO_2]_T$ measured in the seawater by coulometry. These quantitative measurements along with resistance profiles confirm that CO_2 degassing at seawater pH below 6 is dependent on salinity and carbonate concentration.

Finally, quantitative production of H_2 from the cathode measured by real-time gas analysis was verified by independent evaluation.

8.0 MILESTONES

- Successful demonstration and reproducibility of pH profiles and electrical resistance trends of the modified electrochemical cell. The results have provided insight into future cell design.

- Further understanding of the scientific parameters (CO_2 solubility, seawater salinity, seawater temperature, seawater surface area, and vacuum conditions) that effect $[CO_2]_T$ degassing from seawater at pH below 6.

- Successful recovery of H_2 using a standard polyethylene hollow fiber membrane contactor and real-time analysis coincides with independent gas sampling analysis.

- Quantitative recovery of CO_2 gas in real-time coincides with coulometric analysis and independent gas sampling analysis.

9.0 RECOMMENDATIONS FOR FUTURE STUDIES

After these initial evaluations the following studies are recommended:

- Design modifications have been made to a new cell based on manipulating key parameters discussed in equations 17, 18 and 19. The design modifications have been tested in the current skid (March 2012) and are the subject of the next report.

- Systematically determine the role of seawater salinity and temperature on CO_2 solubility in seawater over the entire pH range.

- Develop and test an electrochemical cell at the laboratory scale for the sole purpose of acidifying seawater to recover CO_2. This cell will not be used to produce hydrogen. This technology is becoming more viable for a growing number of processes seeking to increase production efficiencies and reduce their overall carbon foot-print. These processes include enhanced biological carbon fixation and new strategies involving CO_2 in Low Temperature Solidification Processes.

10.0 REFERENCES

[1] "Single Naval Fuel at Sea Feasibility Study – Phase One" NAVAIRSYSCOM Report 445/02-004, October 25, 2002.

[2] Davis, B. H. Topics in *Catalysis* **2005**, *32,* 143-168.

[3] Hardy, D. R. Zagrobelny, M.; Willauer, H. D.; Williams, F. W. *Extraction of Carbon Dioxide From Seawater by Ion Exchange Resin Part I: Using a Strong Acid Cation Exchange Resin*; Memorandum Report 6180-07-9044; Naval Research Laboratory: Washington DC, 20 April 2007.

[4] Willauer, H. D.; Hardy, D. R.; Lewis, M. K.; Ndubizu, E. C.; Williams, F. W. "Recovery of $[CO_2]_T$ from Aqueous Bicarbonate Using a Gas Permeable Membrane" Memorandum Report 6180-08-9129; Naval Research Laboratory: Washington DC, 25 June 2008.

[5] Willauer, H. D.; Hardy, D. R.; Lewis, M. K.; Ndubizu, E. C.; Williams, F. W. Recovery of CO_2 from Aqueous Bicarbonate Using a Gas Permeable Membrane. *Energy & Fuels*, **2009**, *23*, 1770- 1774.

[6] Willauer, Willauer, H. D.; Hardy, D. R.; Lewis, M. K.; Ndubizu, E. C.; Williams, F. W. "Extraction of CO_2 From Seawater By Ion Exchange Resin Part II: Using a Strong Base Anion Exchange Resins" Memorandum Report 6180-09-9211; Naval Research Laboratory: Washington DC, 29 September 2009.

[7] Dorner, R. W.; Hardy, D. R.; Williams, F. W.; Davis, B. H.; Willauer, H. D. Influence of Gas Feed Composition and Pressure on the Catalytic Conversion of CO_2 Using a Traditional Cobalt-Based Fischer-Tropsch Catalyst. *Energy & Fuels*, **2009**, 23, 4190-4195.

[8] Dorner, R. W.; Willauer, H. D.; Hardy, D. R.; Williams, F. W. "Effects of Loading and Doping on Iron-based CO_2 Hydrogenation Catalyst," Memorandum Report 6180-09-9200; Naval Research Laboratory: Washington DC, 24 August 2009.

[9] Dorner, R. W.; Hardy, D. R.; Williams, F. W.; Davis, B. H.; Willauer, H. D. K and Mn doped Iron-based CO_2 Hydrogenation Catalysts: Detection of $KAlH_4$ as part of the catalyst's active phase. *Applied Catalysis A,* **2010**, 373, 112-121.

[10] Dorner, R. W.; Hardy, D. R.; Williams, F. W.; Davis, B. H.; Willauer, H. D. Effects of Ceria-doping on a CO_2 Hydrogenation Iron-Manganese Catalyst. *Catalysis Communications*, **2010**, *11*, 816-819.

[11] Dorner, R. W.; Hardy, D. R.; Williams, F. W.; Davis, B. H.; Willauer, H. D. Heterogeneous catalytic CO_2 conversion to value-added hydrocarbons. *Energy and Environmental Science*, **2010**, *3*, 884-890.

[12] Willauer, H. D.; Hardy, D. R.; Lewis, M. K.; Ndubizu, E. C.; Williams, F. W. The Effects of Pressure on the Recovery of CO_2 by Phase Transition from a Seawater System by Means of Multi-layer Gas Permeable Membranes. *J. Phys. Chem. A,* **2010**,114, 4003-4008.

[13] DiMascio, F.; Willauer, H. D.; Hardy, D. R.; Lewis, M. K.; Williams, F. W. "Extraction of Carbon Dioxide From Seawater By An Electrochemical Acidification Cell Part I. Initial Feasibility Studies," Memorandum Report 6180-10-9274; Naval Research Laboratory: Washington DC, 23 July 2010.

[14] Hardy, D. R. "Sea-based Fuel Synthesis Work at NRL from FY02 to FY07 (October 2001-October 2006)," Memorandum Report 6180-10-9276; Naval Research Laboratory: Washington DC, 5 August 2010.

[15] Willauer, H. D.; DiMascio, F.; Hardy, D. R.; Lewis, M. K.; Williams, F. W. Development of an Electrochemical Acidification Cell for the Recovery of CO_2 and H_2 from Seawater. *Ind. Eng. Chem.*, **2011**, *50*, 9876-9822.

[16] Willauer, H. D.; DiMascio, F.; Hardy, D. R.; Lewis, M. K.; Williams, F. W. "Extraction of Carbon Dioxide from Seawater by an Electrochemical Acidification Cell Part II: Laboratory Scaling Studies" NRL Memorandum Report, 6180-11-9329, 11, April 2011.

[17] Dorner, R. W.; Hardy, D. R.; Williams, F. W., Willauer, H. D. C2-C5+ olefin production from CO2 hydrogenation using ceria modified Fe/Mn/K catalysts. *Catalysis Communications,* **2011**, *15*, 88.

[18] Willauer, H. D.; DiMascio, F.; Hardy, D. R.; Williams, F. W. "Extraction of Carbon Dioxide from Seawater by an Electrochemical Acidification Cell Part III: Scaled –Up Mobile Unit Studies (January and April of 2011)" NRL Memorandum Report, 6300-12-9414, 30 May 2012.

[19] Willauer, H. D.; DiMascio, F.; Hardy, D. R.; Lewis, M. K.; Williams, F. W. Development of an Electrochemical Acidification Cell for Recovery of CO_2 and H_2 from Seawater II. Evaluation of the Cell by Natural Seawater. *Ind. Chem. Res.* DOI: 10.1021/ie301006y, 2 Aug 2012.

[20] Johnson, K. M., King, A. E., Sieburth, J. Coulometric TCO2 Analyses for Marine Studies: An Introduction. Marine Chem. 1985, 16, 61.

[21] Willauer, H. D.; Hardy, D. R.; Williams, F. W. “The Feasibility and Progress of Scaling NRL Technologies for Producing Jet Fuel at Sea Using Carbon Dioxide and Hydrogen” NRL Memorandum Report, 6180-10-9300, 29 September 2010.

[22] Riedel, T; Schaub, G.; Jun, K-W; Lee, K-W. Kinetics of CO_2 Hydrogenation on a K-Promoted Fe Catalyst. *Ind. Eng. Chem Res.* **2001**, *40*, 1355-1363.